

Levels and Transition Rates in ^{53}Mn from the $^{53}\text{Cr}(p,n)^{53}\text{Mn}$ and $^{53}\text{Cr}(p,n\gamma)^{53}\text{Mn}$ Reactions*

J. E. Wiest,† C. Robertson, F. Gabbard, and M. T. McEllistrem

University of Kentucky, Lexington, Kentucky 40506

(Received 18 May 1971)

Differential cross sections of the (p,n) reactions have been measured as a function of angle at several proton energies from 2.6 to 5.9 MeV. Neutron groups corresponding to the ground and 21 excited levels have been observed, and excitation energies fixed to within ± 5 keV in these measurements. The good agreement between the measured cross sections and those calculated in the Wolfenstein-Hauser-Feshbach (WHF) formalism for levels of known spin and the agreement between measured and calculated neutron angular distributions permitted tentative assignments to many levels of unknown spin. Angular distributions of the $(p,n\gamma)$ transitions were measured at 4.9-MeV proton energy, with transitions from 19 excited levels observed. A decay scheme and excitation energies with ± 2 -keV uncertainty were obtained from the γ -ray measurements. Analysis of the angular distributions in the WHF formalism together with the neutron measurements provided the following excitation energies in keV and spin assignments: 2272, ($\frac{5}{2}, \frac{7}{2}$); 2405, ($\frac{3}{2}, \frac{5}{2}$); 2571, ($\frac{7}{2}, \frac{7}{2}$); 2685, ($\frac{7}{2}, \frac{7}{2}$); 2949, ($\frac{3}{2}, \frac{5}{2}$); 3004, ($\frac{3}{2}, \frac{5}{2}$); 3199, ($\frac{5}{2}, \frac{7}{2}, \frac{7}{2}$); 3248, ($\frac{3}{2}, \frac{5}{2}$). Tentative assignments are in parentheses.

The level and decay schemes are in good agreement with mixed-configuration shell-model calculations for the first levels of a given spin. For higher levels the comparison of calculated and measured schemes suggests an inadequate model space in those calculations which allow only one proton excited out of the $f_{7/2}$ shell.

INTRODUCTION

The $^{53}\text{Cr}(p,n)^{53}\text{Mn}$ and the $^{53}\text{Cr}(p,n\gamma)^{53}\text{Mn}$ reactions have been studied to obtain new spectroscopic information on the residual nucleus. The ^{53}Mn nucleus is of special interest because its 28 neutrons form a closed shell. It has 25 protons. Early shell-model calculations by McCullen, Bayman, and Kashy¹ have agreed well with experiment on the energies of low-lying levels of ^{53}Mn . However, those calculations predict only six energy levels in ^{53}Mn while experimental investigators have reported over 30 levels. McCullen, Bayman, and Kashy assumed the 5 protons outside the closed shell of 20 protons to be in the $1f_{7/2}$ shell in which 8 protons are allowed. Recently, Lips and McEllistrem² have included configurations in which one proton is excited out of that shell in effective-interaction calculations. These have improved the agreement between the predicted and measured excitation energies of the low-lying levels and have, of course, yielded many more calculated levels.

Investigators have studied several nuclear reactions in order to measure the properties of the excited levels of ^{53}Mn . Through studies of the $^{52}\text{Cr}(^3\text{He},d)^{53}\text{Mn}$ reactions, three different investigators³⁻⁵ have measured many excitation energies and parities. Two studies^{6,7} of the $^{52}\text{Cr}(p,\gamma)^{53}\text{Mn}$ reaction have permitted excitation-energy measurements and spin assignments. The $^{53}\text{Cr}(p,n\gamma)^{53}\text{Mn}$ reaction study by McEllistrem, Jones, and

Sheppard⁸ has been very successful in measuring the low-lying excitation energies and in assigning unique spins to three of the levels. The $^{52}\text{Cr}(\alpha,t)^{53}\text{Mn}$,⁹ $^{54}\text{Fe}(d,^3\text{He})^{53}\text{Mn}$,¹⁰ and $^{50}\text{Cr}(\alpha,p\gamma)^{53}\text{Mn}$ ¹¹ reaction studies have also given information on the spins and excitation energies of the low-lying states. A previous $^{53}\text{Cr}(p,n)^{53}\text{Mn}$ study was done by Elwyn *et al.*¹² to measure excitation energies of low-lying states. Brown, Warren, and Middleton (BWM)¹³ have reported a large number of energy levels below the excitation energy of 4 MeV from the study of the $^{56}\text{Fe}(p,\alpha)^{53}\text{Mn}$ reactions. Most recently, a high-resolution, high-sensitivity set of measurements¹⁴ of the neutron-energy spectra from the $^{53}\text{Cr}(p,n)^{53}\text{Mn}$ reactions have been made using time-of-flight neutron detection. This experiment illustrated the use of this method of determining level schemes, but was not designed to measure absolute cross sections or angular distributions.

The several experiments cited leave the level scheme of ^{53}Mn defined with confidence through an excitation energy of 3.2 MeV. The spins and lifetimes of the first four excited levels and the branching ratios and multipole mixing ratios of transitions from them are all rather well known, and in good agreement with expectations of mixed-configuration shell-model calculations.²

However, more work on ^{53}Mn and other nuclei is needed in order to present a proper test of the adequacy of the shell-model interpretation. It is

really necessary to reach an excitation energy of 2.5–3.0 MeV to test for the presence of admixed particle configurations which small-space shell-model calculations would miss. The lowest five levels in ^{53}Mn , which have been studied extensively, lie below 1.62-MeV excitation energy.

There were other interesting questions to stimulate the study of the $^{53}\text{Cr}(p, n)^{53}\text{Mn}$ reactions. The Wolfenstein-Hauser-Feshbach¹⁵ (WHF) statistical model has been shown to give a valid picture of (p, n) cross sections on nuclei near mass 90 by Kim and Robinson¹⁶ and Dutt and Gabbard.¹⁷ The only previous statistical-model analysis of a (p, n) reaction in the mass-50 region was the $^{51}\text{V}(p, n)^{51}\text{Cr}$ study by Egan *et al.*¹⁸ In their study of the $^{53}\text{Cr}(p, n\gamma)^{53}\text{Mn}$ reactions, McEllistrem, Jones, and Sheppard⁹ measured γ -ray angular distributions and (p, n) cross-section ratios and used both in an analysis which yielded several unique spin assignments and properties of the transitions. However, they did not measure absolute cross sections, a severe test of the adequacy of the WHF model.

The present work includes measurements of total neutron-production cross sections as a function of proton energy, of differential cross sections as a function of angle and proton energy, and of γ -ray angular distributions and branching ratios. From the neutron data we confirm the level scheme of Tanaka *et al.*¹⁴ and of other workers.¹³ From the neutron excitation functions and the absolute cross sections to levels of known spin, we are

able to confirm the validity of the WHF model at high proton energies and away from resonances. The neutron and γ -ray angular distributions are the basis for several spin assignments, and the γ -ray data yield a decay scheme, including branching ratios and some mixing ratios for mixed-multipole transitions.

The approach taken for the WHF analysis of the neutron cross sections was to search for a proton energy region free of any large cross-section fluctuations, to measure several angular distributions in that region, and to average the angular distributions. The applicability of the model was checked by comparing the cross-section magnitudes and angular-distribution shapes with statistical-model calculations for neutrons leaving ^{53}Mn in the first five energy levels which had been well established both in excitation energy and in spin assignment.

EXPERIMENTAL PROCEDURE

The $^{53}\text{Cr}(p, n)^{53}\text{Mn}$ reactions were studied using a Hanson and McKibben long counter¹⁹ and a proton-recoil scintillator with time-of-flight techniques for neutron detection. The long-counter yields included neutron groups to all energetically allowed final levels and were obtained for proton excitation functions at 20 and 110°. The 20° yields covered the proton energy range from 2.4 to 5.9 MeV and the 110° yields were measured from 2.4 to 4.4 MeV.

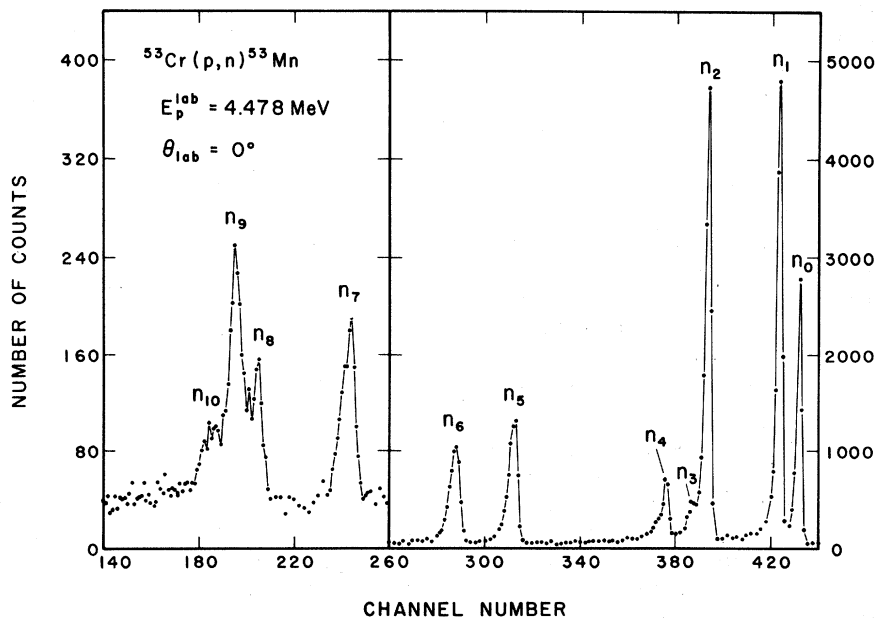


FIG. 1. Time-of-flight spectrum of neutrons corresponding to the ground and first 10 excited states of ^{53}Mn . For the correspondence between group number and level excitation energy, see Table I.

The time-of-flight measurements employed $\frac{1}{2}$ -in.- and 2-in.-thick by 4-in.-diam liquid scintillators. These measurements were designed to separate the neutron groups to different final levels. The proton beam was pulsed at the terminal of the 5.5-MeV accelerator to pulses of 7–10-nsec width at a repetition rate of 2 MHz and bunched after acceleration to pulses of <1-nsec width. The time-of-flight methods were generally very similar to those of Egan *et al.*²⁰

Targets of Cr_2O_3 were evaporated onto thin aluminum foils and 15-mil-thick tantalum disks. The targets on thin foil backings were used in a scattering chamber to obtain yields of protons elastically scattered from ^{53}Cr as a function of scattering angle and at low proton energies. Since the measured angular dependence was that of Coulomb scattering, the target thickness was ascertained from the scattering yields assuming the Coulomb-scattering cross sections. The thicknesses of the targets on Ta disks were then determined by comparing yields of neutrons from them with those from the Al-backed targets, using the long counter to measure the neutron yields from both targets. Two thicknesses of Cr_2O_3 targets were prepared, 34 and $345 \mu\text{g}/\text{cm}^2$. The targets were 1.5 and 15 keV thick, respectively, to 5-MeV incident protons. The 1.5-keV target was used for good precision in the time-of-flight neutron-energy measurements, to be discussed below. The 15-keV target was used for neutron angular-distribution measurements.

The γ -ray angular distributions were measured

with a shielded 35-cm^3 Ge(Li) detector mounted on a rotatable carriage whose axis of rotation passed through the center of the target. Target-to-detector distance was set at 60 cm and the measurements were completed using pulsed-beam time-of-flight techniques often used in this laboratory in connection with $(n, n'\gamma)$ reaction studies.²¹ The measurements were taken for nine angles between 15 and 145° with respect to the incident proton beam and at an incident energy of 4.9 MeV. The $345\text{-}\mu\text{g}/\text{cm}^2$ target was used for these data and the yields were corrected for absorption in the target backing and other material between target and detector at backward angles. The yields were also corrected for deadtime and γ -ray detection efficiency. The corrected angular distributions were least-squares-fitted to the form

$$W(\theta) = A_0 [1 + a_2 P_2(\cos \theta) + a_4 P_4(\cos \theta)].$$

RESULTS AND ANALYSIS

A. Excitation Energies

The excitation energies of ^{53}Mn were determined through the measurement of flight times of neutrons from the $^{53}\text{Cr}(p, n)^{53}\text{Mn}$ reactions and from the measurement of γ -ray energies from the $^{53}\text{Cr}(p, n\gamma)^{53}\text{Mn}$ reactions. Individual neutron groups were studied in time spectra for different flight distances, different incident proton energies, and different scattering angles. A thin target, a bunched proton pulse <1 nsec wide, a thin scintillator, and a constant fraction pulse-height trigger²² on the

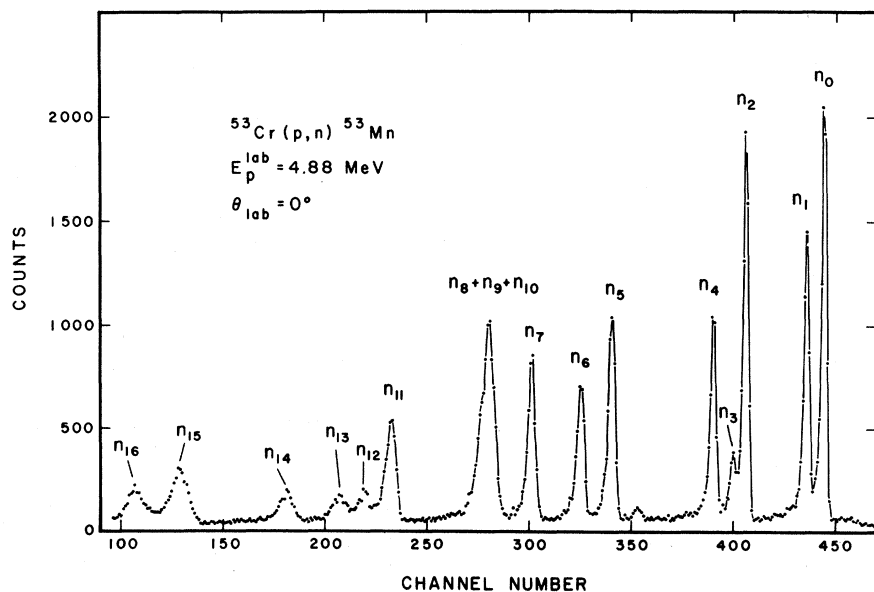


FIG. 2. Time-of-flight spectrum of neutrons corresponding to the ground and first 16 excited states of ^{53}Mn . For the correspondence between group number and level excitation energy, see Table I.

anode pulse from the photomultiplier tube of the neutron detector were important factors in neutron-group time resolution. Good resolution permitted a short neutron flight distance so that one time spectrum with good counting statistics on many neutron groups could be measured in a reasonably short running time. Typical time spectra are shown in Figs. 1 and 2.

The time-of-flight system was calibrated in time by using four energy levels in ^{53}Mn that had previously been determined with uncertainties equal to or less than 2 keV. The energy levels are the ground state, the 1619.1 ± 0.3 -keV level,⁸ the 2571 ± 2 -keV level, and the 3095 ± 2 -keV level. The latter two energies are from the present ($p, n\gamma$) determinations. The ground-state Q value for the present reaction had been previously measured²³ to be 1380.4 ± 1.6 keV. The energies of the incident protons were calibrated in reference to the threshold of the $^7\text{Li}(p, n)^7\text{Be}$ reaction at 1881.4 ± 0.1 keV.²⁴ The flight times over measured distances for neutrons leaving ^{53}Mn in the above four energy levels were calculated from the above information. The time per channel was calculated between each successive pair of groups to the above energy levels assuming system linearity between each pair.

The flight time of each neutron group was determined from its channel position and the calibration of the system. Since there was some overlapping among neutron groups in the time spectra, the Tepel²⁵ method for unfolding overlapping peaks was employed in order to determine the centroid of each neutron group accurately. A time spectrum from the $\text{T}(p, n)^3\text{He}$ reaction was used as a reference peak to fit the shape of each overlapping peak. The backgrounds in the time spectra were fitted with parabolas; and the height, width, and position of the peaks were varied until a good fit to the entire time spectrum of the reaction under study was obtained. The energy of an unknown neutron group was calculated from its determined flight time, and the Q value of the corresponding excited state of ^{53}Mn was calculated from the neutron-group energy and the incident proton energy. The excitation energy of the observed state was then calculated as the ground-state Q value minus the excited-state Q value. The estimated error in the excitation-energy determinations is ± 5 keV. Neutrons leaving ^{53}Mn in the ground state and 21 excited states were observed.

γ rays from 19 excited levels of ^{53}Mn were observed. All but five of these decay to ground and most of them were found to decay also to one or more of the first few excited levels. The energies of the γ rays were determined by using as internal calibration lines the 564.1-keV line of ^{53}Cr and the

^{53}Mn lines at 910.8, 1288.4, and 1619.1 keV. These energies were measured by McEllistrem, Jones, and Sheppard⁸ and have uncertainties of ± 0.3 keV.

The present work verifies all states reported by BWM¹³ in their studies of the $^{54}\text{Fe}(p, \alpha)^{53}\text{Mn}$ reactions and by Tanaka *et al.* in their measurements of neutron energies from the $^{53}\text{Cr}(p, n)$ reactions.¹⁴ In fact all levels observed in the present study were reported in Ref. 14 and good agreement exists between the present energy measurements and their measurements. A doublet was reported near 2689 keV by BWM¹³ and others.⁵ The level scheme determined in the present work is that implied by the neutron spectra of Figs. 1 and 2. The neutron groups to the different excited levels of ^{53}Mn are indicated by group numbers in these spectra, and the correspondence between group number and residual level excitation energy is given in Table I. In the present work, three states were observed with excitation energies near 2669, 2687, and 2705 keV. The corresponding neutron groups are shown in Fig. 1 and are labeled n_8 , n_9 , and n_{10} . The energy levels near 2913 and 3190 keV reported in the present work are confirmations of levels reported by Vuister.⁷ The neutron group corresponding to the 2913-keV level is shown in Fig. 2 and is labeled n_{12} . The present work observed two states with excitation energies of 3095 and 3124 keV which correspond to the neutron groups labeled n_{15} and n_{16} in Fig. 2. BWM¹³ and other investigators reported only one state, with an excitation energy of 3109 keV. For states that have excitation energies above 3124 keV there is good agreement between the present work and the work of BWM.¹³ In the excitation-energy range from 3150 to 3600 keV, investigators of the $^{52}\text{Cr}(^3\text{He}, d)^{53}\text{Mn}$ reactions reported only a state near 3496 keV which is confirmed in the present work. Five neutron groups corresponding to states in that energy region are observed and labeled n_{17} through n_{21} , but are not shown in Figs. 1 and 2.

Several criteria have been used in the present work to decide if a neutron peak in the time spectrum belongs to ^{53}Mn . A neutron group could be distinguished from γ rays by observation of the time spectrum at different flight distances for a constant incident proton energy. Since the γ rays travel at the speed of light, their channel positions will change only 3.33 nsec for a change in flight distance of 1 m, whereas the much slower neutrons will change more rapidly in their channel positions. Impurities of isotopes other than ^{53}Cr in the target were looked for in the elastic scattering of protons from a target on a thin carbon backing. The pulse-height spectrum showed contaminants of oxygen and an isotope of high atomic number. The latter impurity is thought to be tantalum, since the Cr_2O_3

was evaporated from a tantalum boat, and the boiling points of the two materials are close. However, such a high- Z material has a low (p, n) cross section because of a high Coulomb barrier at energies used in the present work. This work was done at lower proton energies than the threshold of the $^{16}\text{O}(p, n)^{16}\text{F}$ reaction. Neutron groups were observed at different incident proton energies and checked for any shift in energy relative to the energy of the ground-state neutrons which would

TABLE I. Excitation energies (E_x), γ -ray energies (E_γ), and branching ratios for the decay of levels of ^{53}Mn . The second column presents the designation of the neutron group to the indicated level, as used in Figs. 1, 2, 5, and 6.

E_x (keV)	Group No.	E_γ (keV)	Branching ratios	
			Present	(Ref. 8)
378	n_1	378	100	100
1288.5	n_2	1288.5	60 \pm 1	57 \pm 1
		910.5	40 \pm 1	43 \pm 1
1440	n_3	1440	100	100
1619	n_4	1619	89 \pm 1	89 \pm 1
		1241	11 \pm 1	11 \pm 1
2272	n_5	2272	77.5 \pm 1	
		1894	22.5 \pm 1	
2405	n_6	2405	39 \pm 3	
		2027	15 \pm 3	
		1116	46 \pm 3	
2571	n_7	2571	41.5 \pm 2	
		2194	58.5 \pm 2	
2669	n_8	2291	48 \pm 2	
		1381	52 \pm 2	
2685	n_9	2685	77 \pm 3	
		2307	14 \pm 3	
		1397	9 \pm 3	
2705	n_{10}	1416	100	
2875	n_{11}	2875	16 \pm 1	
		2497	84 \pm 1	
2911	n_{12}	2533	100	
2949	n_{13}	2949	100	
3004	n_{14}	3004	24 \pm 3	
		2626	76 \pm 3	
3095	n_{15}	3095	36 \pm 2	
		2717	48 \pm 2	
		1476	16 \pm 2	
3124	n_{16}	2746	100	
3180		2802	100	
3199	n_{17}	3199	54 \pm 3	
		2821	46 \pm 3	
3248	n_{18}	3248	100	

characterize neutrons corresponding to a residual nucleus different from that of ^{53}Mn .

B. Cross Sections

The experimental total neutron-production cross sections were compared with calculations of the absorption cross section for a complex potential. Transmission coefficients were calculated for the potential using a computer code written by Smith.²⁶ The code was modified to give directly the absorption cross section.

The comparison between the (p, n) experimental data and the theoretical calculations, the smooth curve, is shown in Figs. 3 and 4. The optical-model parameters of Rosen,²⁷ which are shown in Table II, were used. This calculation actually predicts the sum of all reaction-product cross sections, but neutrons dominate in the proton energy range shown. Calculations with the WHF statistical model predict that neutrons account for the following percentages of the total reaction cross section at the incident proton energies cited: 94% at 3.0 MeV, 85% at 4.5 MeV, and 80% at 6.0 MeV. The error bars shown in Fig. 4 are relative errors of $\pm 10\%$; absolute errors are estimated to be $\pm 20\%$. The curves plotted in Figs. 3 and 4 should reflect

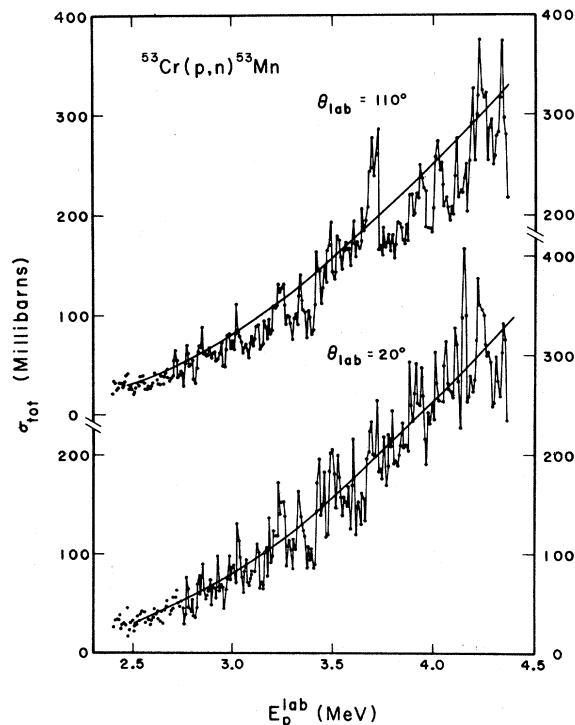


FIG. 3. Excitation functions of the total neutron cross section. Neutron yields at two scattering angles are compared. Solid curves are optical-model calculations with Rosen parameters.

the fact that the (p, n) cross sections do not exhaust the total reaction cross section, as indicated by the cross-section percentages given above. Corrections for this have not been made, however, because the measured cross sections have uncertainties at least as large as the indicated corrections. The corrections would have to depend on the WHF or other model, and be somewhat uncertain for this reason. The curves in Figs. 3 and 4 are the calculated total reaction cross sections which depend only on the Rosen potential. The measured total cross sections shown are actually inferred from large-angular-spread measurements at two angles. The energy averages of the two sets of measured values are the same, as is apparent in Fig. 3, and this illustrates the approximate isotropy of the (p, n) cross sections when the measurements include all outgoing neutron groups. The agreement between measured and calculated cross sections is quite impressive, since parameter adjustments to modify the potential to fit the present data were not made.

Angular distributions of neutrons leaving ^{53}Mn in different energy levels were measured in three different incident-proton-energy regions. The mea-

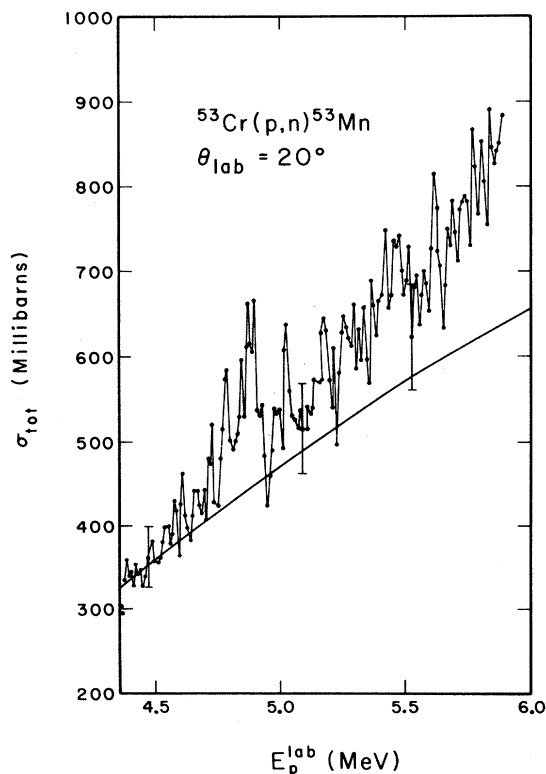


FIG. 4. Excitation function of the total neutron-production cross section for higher incident proton energies. Solid curve is an optical-model calculation with Rosen parameters.

surements were done in regions free of any large cross-section fluctuations and were energy averaged by measuring several angular distributions in incident-proton-energy steps equal to the target thickness and then averaging the different angular distributions. The three mean proton energies represent energy averages of 30, 45, and 70 keV, respectively. Overlapping peaks were unfolded by the Tepel method as described previously. Results at the highest proton energy are shown in Figs. 5 and 6. The (p, n) cross sections are thus obtained from two independent sets of measurements, one set measured with a long counter which had been calibrated with standard neutron sources and the other set measured with time-of-flight neutron detection using a liquid scintillation proton-recoil detector. The two sets of measurements agreed to within 15%.

Calculations of the differential cross sections were made in the WHF formalism and are shown with the data in Figs. 5 and 6. Several different sets of published optical-model parameters were tried,²⁷⁻³¹ and the effect of parameter variation on the magnitude and shape of the angular distributions was observed. The shapes were essentially independent of parameter changes, but the magnitudes show considerable dependence upon the potential parameters.

As noted above, Rosen²⁷ proton and neutron parameters gave closest agreement to the data at all three incident proton energies and are used for the curves shown in the figures. The neutron parameters of Chung *et al.*³¹ substituted for the Rosen neutron parameters gave the same results as those in Figs. 5 and 6 to within $\pm 4\%$. The parameter sets and the optical-model potentials used in the present calculations are given in Table II. $V_{ES}(r)$ is the Coulomb potential. In the work of Egan *et al.*¹⁸ on the $^{51}\text{V}(p, n)^{51}\text{Cr}$ reaction, the success of the statistical model was shown to improve in increasing the incident proton energy from 4 to 5 MeV. This case is similar. At the proton energy of 5.724 MeV there is good agreement between the measured data and the theoretical calculations.

At 5.724 MeV there is agreement between the measured and the theoretical cross sections for the ground state at all angles greater than 30° within the experimental error in the absolute cross section, which is twice the relative error shown. The good agreement with the statistical model for the ground and first four excited levels, for which the spins are known,⁸ suggests that the requirements of the statistical model are satisfied in this energy region so that properties of the higher excited states can be investigated by use of this reaction model. Such an investigation led to the results plotted with the higher excited states. The

results are discussed below. Figures 5 and 6 show calculations with the Rosen parameters for states of known spin and then several calculations assuming different spins for states where the spin is unknown or where there is uncertainty. It is important to point out that there is no normalization of the theoretical calculations to any of the experimental data. The experimental data have an absolute error of $\pm 15\%$ and relative errors of 7.5 to 9%.

C. γ -Ray Results

The identification of the ^{53}Mn transitions from the $(p, n\gamma)$ reactions was made for most lines by observing them in coincidence with neutrons. The Ge(Li) detector and a 5-cm \times 5-cm liquid scintillation proton-recoil detector were both mounted at 90° to the beam direction and at 90° from each other with respect to the target. Almost all of the transitions reported here with energies below 2750 keV were identified in this way. The positions of the transitions in the level scheme were fixed by measuring γ -ray yields as a function of incident proton energy and observing thresholds for the production of the transitions. Some threshold determinations and their use are illustrated⁸ in the earlier $(p, n\gamma)$ study.

The γ -ray angular distributions from the $(p, n\gamma)$ reactions, with neutrons unobserved, provide a nearly reaction-independent test of the spins of the emitting levels and the multipolarity of the transitions. The γ -ray anisotropies are almost completely independent of the mechanism of reactions populating the states and have, in fact, been used in two experiments^{7,8} to obtain several spin assignments and multipole-mixing ratios for levels and transitions in ^{53}Mn . As noted in an earlier section, transitions from 19 levels were observed in this

work, and most of these were observed to decay to two or more levels. Angular distributions were measured between 15 and 145° and corrected for counting losses caused by dead time, for absorption in the target and surrounding materials, and for the efficiency of the Ge(Li) detector. From the corrected distributions we obtained branching ratios for the decay of excited levels, and these are given with the excitation and transition energies in Table I. A few of the ratios duplicate measurements of Ref. 8, and the agreement between the two sets of measurements is excellent.

The angular distributions have been fitted to an expansion in Legendre polynomials using the least-squares procedure, and fits are shown with the measured distributions in Figs. 7 and 8 as solid curves. Table III presents the anisotropy coefficients, a_2 and a_4 . Since the first excited level is heavily fed by cascade γ rays, it would be necessary to correct the angular distributions of the 378-keV line for these cascades in order to have an anisotropy which would yield information about the 378-keV transition. Since this line has been studied without cascades present,⁸ the uncertain cascade corrections to the present data were not made.

The distributions were analyzed in the WHF formalism as in Ref. 8, with transmission coefficients obtained from appropriate complex potentials for the proton and neutron channels. The proton potential parameters were the Rosen parameters²⁷ already mentioned and the neutron parameters were those of Chung *et al.*³¹ Other choices for proton potentials were also tested, but the results were not appreciably altered by different choices of potentials. The calculated angular distributions depend on assumed values of spins for the emitting levels and on the mixing ratios δ for those transitions which admit multiplicity mixtures. The

TABLE II. Form of optical-model potential and parameters used in calculations of transmission coefficients.

Parameter	Rosen Protons (7-22 MeV)	Neutrons (0.2-24 MeV)	Perey Protons (9-22 MeV)	Perey and Buck Neutrons (1-25 MeV)	Chung <i>et al.</i> Neutrons (0.5-2.0 MeV)
V (MeV)	$53.8-0.33E$	$49.3-0.33E$	$53.3-0.55E$ $+0.4\frac{Z}{A^{1/3}}+27\frac{N-Z}{A}$	$48-0.29E$	46
W (MeV)	7.5	5.75	13.5	9.6	$2.5+E$
R (F)	$1.25A^{1/3}$	$1.25A^{1/3}$	$1.25A^{1/3}$	$1.27A^{1/3}$	$1.16A^{1/3}$ $+0.60$
a (F)	0.65	0.65	0.65	0.66	0.65
b (F)	0.70	0.70	0.47	0.47	0.50
V_s (MeV)	5.5	5.5	7.5	7.2	7.0

$$V = V_{ES}(r) - V \frac{1}{1 + e^{(r-R)/a}} - iW \frac{d}{dr} \frac{4b}{1 + e^{(r-R)/b}} + \left(\frac{\hbar}{M\pi c} \right)^2 \frac{V_s}{r} \frac{d}{dr} \frac{1}{1 + e^{(r-R)/a}} \vec{1} \cdot \vec{\sigma}; R = r_0 A^{1/3}.$$

procedure followed was to vary δ to obtain a best fit of the theoretical calculation to the measured distributions, using the usual Q^2 criterion³ to define goodness of fit. Results are given below, for each level, of the combined analysis of the neutron angular distributions, (p, n) cross sections, and γ -ray angular distributions.

2272-keV level. The spin of this level was unknown. The fact that several studies³⁻⁵ of the $^{52}\text{Cr}-(^3\text{He}, d)^{53}\text{Mn}$ reaction did not report this level suggests that it may have high spin, since these single-nucleon-transfer reactions also missed the $\frac{11}{2}$ and $\frac{9}{2}$ levels at 1440 and 1619 keV. In the present analysis, all possible spins were considered in the WHF calculations, but only three gave neutron differential cross sections close to those observed for the n_5 group shown in Fig. 5. The generally good agreement between measured and calculated cross sections in Fig. 5 and the fact that a $\frac{9}{2}$ assignment gives values low by almost a factor of 2 argues against that assignment. The analysis of the γ -ray transition to the ground state would admit any spin between $\frac{5}{2}$ and $\frac{9}{2}$, but the fit to the 1894-keV cascade to the first excited state permits only $\frac{5}{2}$ or $\frac{7}{2}$,

with $\frac{7}{2}$ favored. This evident in the Q^2 , or goodness of fit, plot shown in Fig. 9 for the 1894-keV transition. The theoretical curves for both $\frac{5}{2}$ and $\frac{7}{2}$ are shown in Fig. 7 together with the measured angular distribution. The $\frac{7}{2}$ curve is indistinguishable from the least-squares fit. The $M1, E2$ mixing ratios of the transition for a $\frac{5}{2}$ or $\frac{7}{2}$ assignment are listed in Table III. The mixing ratio δ is defined to be $\delta \equiv \langle |L+1| \rangle / \langle |L| \rangle$, with the phase convention of Rose and Brink.³² Recent work by Szöghy, Cujec, and Dayras³³ results in a $\frac{5}{2}$ assignment to the level.

2405-keV level. This level is strongly excited in stripping^{4,5} and pickup¹⁰ reaction studies as an $l=1$ transition, and is presumed to be $\frac{3}{2}^-$, with a substantial fraction of the $2p_{3/2}$ single-particle strength. The only possible spins are $\frac{1}{2}$ and $\frac{3}{2}$, and the neutron cross sections, n_6 of Fig. 5, strongly favor $\frac{3}{2}^-$. The fact that three γ rays from the level are approximately isotropic is consistent with either a $\frac{1}{2}$ or $\frac{3}{2}$ assignment.

2571-keV level. This is another level not observed in the previously cited single-nucleon-transfer studies, so it also probably has $J \geq \frac{5}{2}$. The anisotropy of the 2571-keV transition is con-

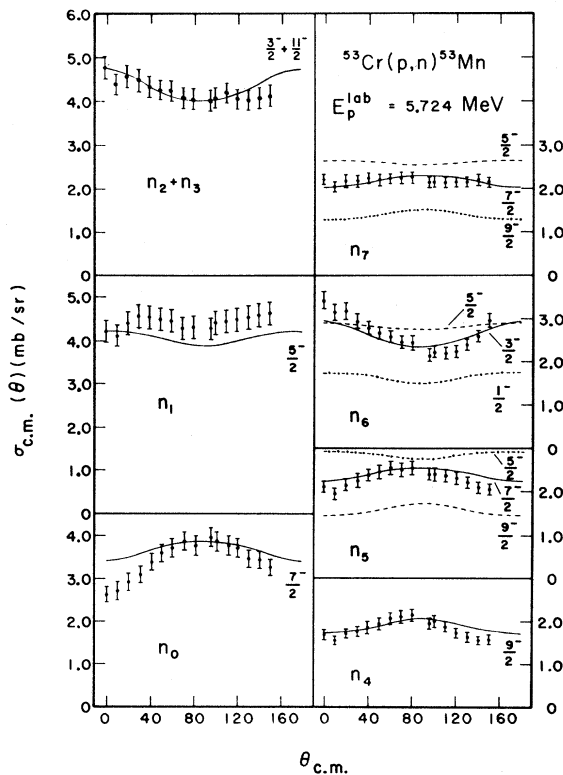


FIG. 5. WHF statistical-model calculations compared with the angular distributions of neutrons corresponding to the ground and first seven excited states of ^{53}Mn . For the correspondence between group number and level excitation energy, see Table I.

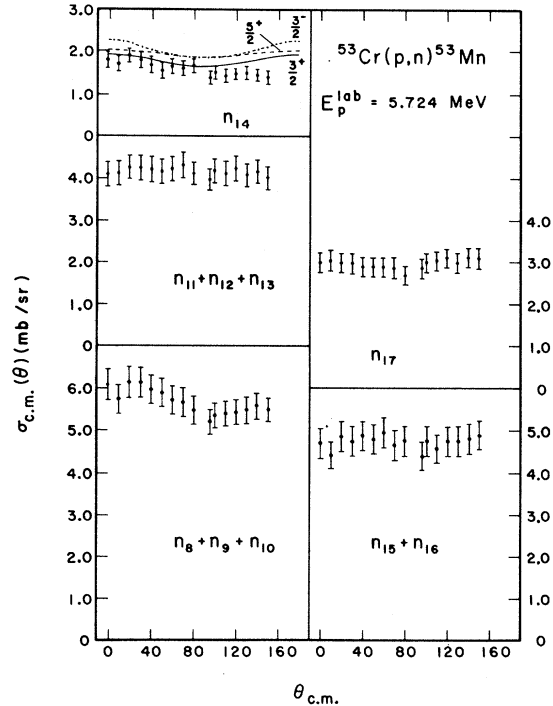


FIG. 6. Angular distributions of neutrons corresponding to the 8th through 17th excited states of ^{53}Mn . WHF statistical-model calculations are compared with the angular distributions of neutrons corresponding to the 14th excited state of ^{53}Mn . For the correspondence between group number and level excitation energy, see Table I.

sistent with spins $\frac{5}{2}^- - \frac{9}{2}^-$, but that of the 2194-keV cascade to the first excited level admits only $\frac{7}{2}^-$ or $\frac{9}{2}^-$. The neutron cross sections for the n_γ group in Fig. 5 discriminate against the $\frac{9}{2}^-$ assignment by almost a factor of 2. The fits to the 2194-keV γ -ray transition also favor $\frac{7}{2}^-$ rather than $\frac{9}{2}^-$. Thus the spin must be $\frac{7}{2}^-$ or $\frac{9}{2}^-$, with $\frac{7}{2}^-$ the most probable assignment. For this assignment, the $M1$, $E2$ mixing ratios are listed in Table III.

The triplet of states observed in this experiment at 2669, 2685, and 2705 keV were not resolved in the (p, n) data at 5.724-MeV proton energy. Angular distributions were obtained for γ rays from the 2669- and 2685-keV levels. Two of the states were excited in single-nucleon-transfer reac-

tions,^{3,5} and they have been assigned as $\frac{1}{2}^-$ and $\frac{1}{2}^+$ levels in two separate experiments.^{4,9}

2669-keV level. Two γ -ray transitions from this level were observed with energies of 1381 and 2291 keV. The stronger line at 1381 keV is isotropic, which is quite consistent with the proposed $\frac{1}{2}^-$ assignment for this level, as are the facts that the dominant decay mode is to the $\frac{3}{2}^-$ level and no decay is observed to the ground state.

2685-keV level. This level decays by ground-state and first-excited-level transitions, both of which were analyzed in the WHF formalism. As

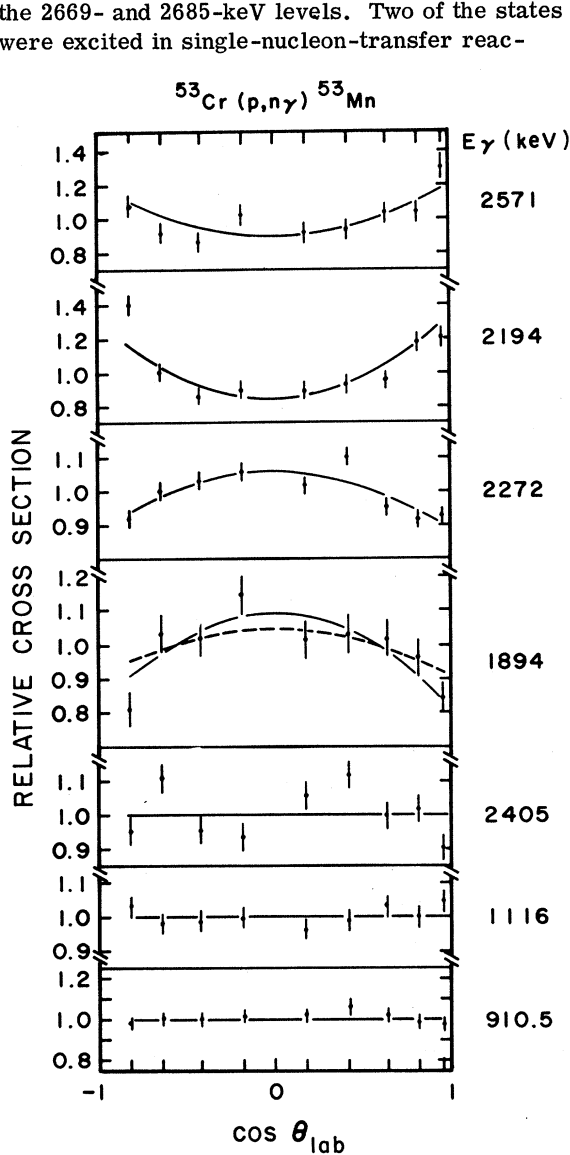


FIG. 7. Angular distributions of γ rays. Solid curves are least-squares fits to the data. Dashed curve for the 1894-keV transition represents WHF theoretical calculations for a spin- $\frac{3}{2}$ assignment for the 2272-keV level.

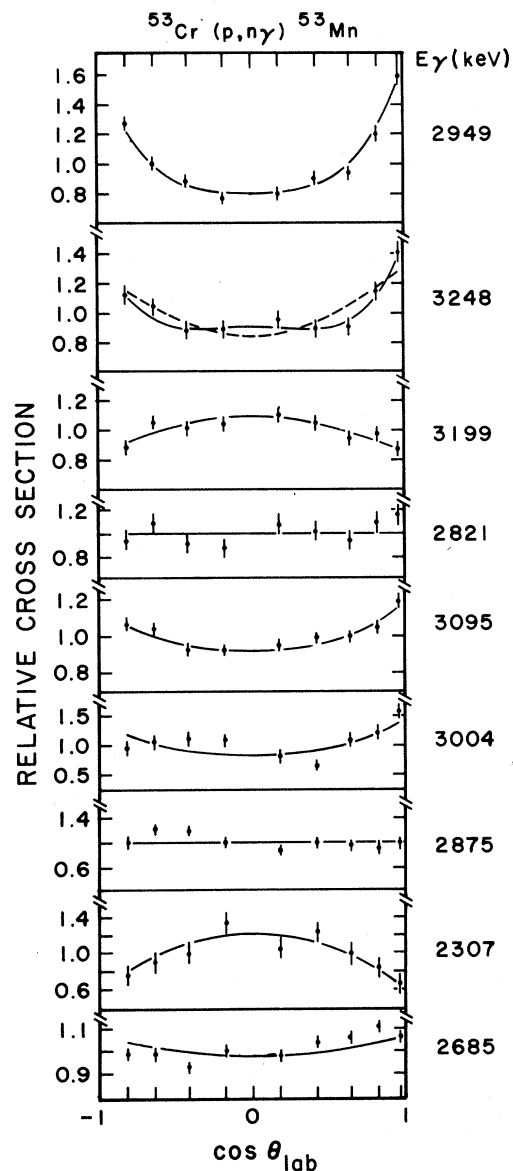


FIG. 8. Angular distributions of γ rays. Solid curves are least-squares fits to the data. Dashed curve for the 3248-keV transition is the best P_2 fit to the data.

TABLE III. Mixing ratios δ and coefficients of least-squares fits to $W(\theta) = A_0[1 + a_2P_2(\cos\theta) + a_4P_4(\cos\theta)]$, for various γ rays. E_i is the energy of the level emitting the γ rays. J_i and J_f are the spins of the initial and final levels of the transition.

E_γ (keV)	E_i (keV)	J_i	J_f	a_2	a_4	δ
378	378	$\frac{5}{2}$	$\frac{1}{2}$		0.0	
910.5	1288.5	$\frac{3}{2}$	$\frac{5}{2}$	0.0	0.0	
1116	2405	$\frac{3}{2}$	$\frac{3}{2}$	0.0	0.0	$\delta \leq 0.5$
1241	1619	$\frac{9}{2}$	$\frac{5}{2}$	0.0	0.0	
1288.5	1288.5	$\frac{3}{2}$	$\frac{1}{2}$	0.0	0.0	
1381	2669	$(\frac{1}{2})$	$\frac{3}{2}$	0.0	0.0	
1440	1440	$\frac{11}{2}$	$\frac{1}{2}$	0.22 ± 0.01	0.0	0.03 ± 0.07
1476	3095		$\frac{9}{2}$	0.0	0.0	
1619	1619	$\frac{9}{2}$	$\frac{1}{2}$	0.20 ± 0.01	0.07 ± 0.014	$-3.7^{+0.5}_{-1.4}$
1894	2272	$(\frac{1}{2})$	$\frac{5}{2}$	-0.18 ± 0.02	0.0	0.09 ± 0.1 or 3.4 ± 1.3
1894	2272	$(\frac{5}{2})$	$\frac{5}{2}$	-0.18 ± 0.02	0.0	3.3 ± 2.4
2027	2405	$\frac{3}{2}$	$\frac{5}{2}$	0.0	0.0	$\delta \leq 0.4$
2194	2571	$(\frac{7}{2})$	$\frac{5}{2}$	0.31 ± 0.03	0.0	$-0.9^{+0.3}$
2272	2272	$(\frac{7}{2})$	$\frac{1}{2}$	-0.12 ± 0.01	0.0	$\delta \geq 0.9$
2272	2272	$(\frac{5}{2})$	$\frac{1}{2}$	-0.12 ± 0.01	0.0	$\delta \leq -0.2$
2291	2669	$(\frac{1}{2})$	$\frac{5}{2}$	0.0	0.0	
2307	2685	$\frac{7}{2}$	$\frac{5}{2}$	-0.42 ± 0.03	0.0	1.5 ± 1.5
2405	2405	$\frac{3}{2}$	$\frac{1}{2}$	0.0	0.0	
2487	2875	$\frac{3}{2}$	$\frac{5}{2}$	0.0	0.0	
2533	2911		$\frac{5}{2}$	0.0	0.0	
2571	2571	$(\frac{7}{2})$	$\frac{1}{2}$	0.20 ± 0.03	0.0	-0.6 ± 0.7
2626	3004	$(\frac{3}{2}, \frac{5}{2})$	$\frac{5}{2}$	0.0	0.0	
2685	2685	$\frac{7}{2}$	$\frac{1}{2}$	0.060 ± 0.015	0.0	$-2.1^{+0.4}_{-0.8}$ or 0.32 ± 0.11
2717	3095		$\frac{5}{2}$	-0.005 ± 0.01		
2746	3124		$\frac{5}{2}$	0.0	0.0	
2802	3180		$\frac{5}{2}$	0.0	0.0	
2821	3199	$(\frac{5}{2}, \frac{7}{2}, \frac{9}{2})$	$\frac{5}{2}$	0.0	0.0	
2875	2875	$\frac{3}{2}$	$\frac{1}{2}$	0.0	0.0	
2949	2949	$\frac{9}{2}$	$\frac{1}{2}$	0.52 ± 0.01	0.16 ± 0.02	-1.6 ± 0.8
3004	3004	$(\frac{3}{2}, \frac{5}{2})$	$\frac{1}{2}$	0.37 ± 0.06	0.0	
3095	3095		$\frac{1}{2}$	0.17 ± 0.01	0.0	
3199	3199	$(\frac{5}{2}, \frac{7}{2}, \frac{9}{2})$	$\frac{1}{2}$	-0.15 ± 0.01	0.0	
3248	3248	$(\frac{9}{2})$	$\frac{1}{2}$	0.31 ± 0.02	0.19 ± 0.02	$-4.5^{+1.9}_{-3.1}$

in several other cases, spin assignments $\frac{5}{2}^- - \frac{9}{2}^-$ provided reasonable fits to the ground-state transition. As is apparent in Fig. 9, however, all spins other than $\frac{7}{2}^-$ are completely ruled out by the 2307-keV transition to the first excited level. The assignment $\frac{7}{2}^-$ is definite for that level. Beyond this excitation energy the neutron-detection data, shown in Fig. 6, cannot be used to discriminate between spin assignments to levels.

2949-keV level. This is the next level for which

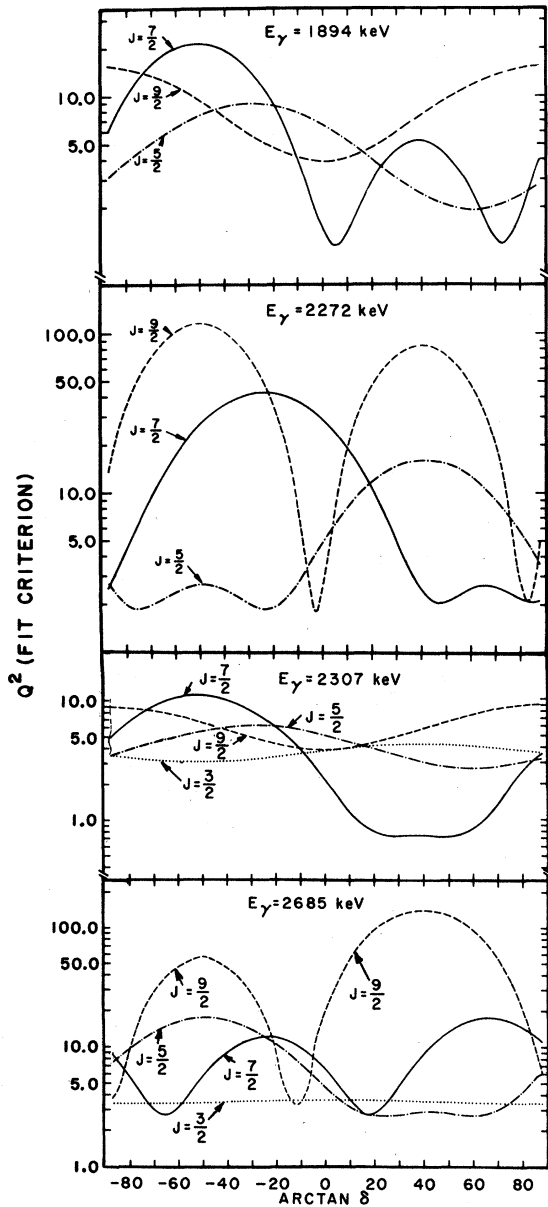


FIG. 9. Goodness-of-fit criterion, Q^2 , vs δ for γ rays deexciting two levels of ^{53}Mn . The WHF calculations fit the data best at minimum values of Q^2 , providing a method of determining δ .

a useful γ -ray angular distribution has been obtained, and is only one of three transitions to show a large a_4 coefficient, as indicated in Table III. As pointed out in earlier work,⁸ this is a unique signature of a $\frac{9}{2}^- \rightarrow \frac{7}{2}^-$ transition, and the Q^2 calculations show that only a $\frac{9}{2}^-$ assignment comes even remotely close to representing the data. Another transition with large a_4 is the 1619.1-keV ground-state transition from the first $\frac{9}{2}^-$ level. Both $\frac{9}{2}^-$ levels decay predominantly to the ground state.

3095-keV level. This level decays to ground, the first excited $\frac{5}{2}^-$ level, and the $\frac{9}{2}^-$ level at 1619 keV. The latter two transitions are nearly isotropic, and all three can be fitted with any spin from $\frac{5}{2}^- - \frac{11}{2}^-$.

3199-keV level. Decay is observed to the ground and first excited levels. The anisotropy of the line to the ground state can be fitted with any J assignment between $\frac{5}{2}^-$ and $\frac{9}{2}^-$ for this level.

3248-keV level. This is the third level which decays predominantly to the ground state and whose decay transition is best fitted with a large a_4 coefficient. Unfortunately the relative uncertainties of the angular-distribution measurements are not as small as those for the 1619.1- and 2949-keV transitions. Thus although a $\frac{9}{2}^-$ assignment provides the only good fit to the 3248-keV line, a $\frac{7}{2}^-$ assignment does have about 10% probability of being correct; it cannot be completely eliminated. A tentative assignment of $\frac{9}{2}^-$ is made to the level.

Other levels and transitions. A single transition of 1417 keV is observed to deexcite the level identified in the (p, n) neutron spectra at 2705 keV. Isotropic cascades are also observed from levels identified in the (p, n) neutron spectra at 2914 and 3124 keV. Since these levels do not decay directly to the ground state and have isotropic transitions to a $\frac{3}{2}^-$ level, they probably have spins $< \frac{7}{2}^-$. The 3004-keV level has been assigned as $\frac{3}{2}^+$ by Newman and Hiebert.¹⁰ The neutron differential cross sections, n_{14} in Fig. 6, and the 2626-keV cascade to the first excited level are well represented by that assignment.

The level and decay schemes for ^{53}Mn resulting from this and earlier work are shown in Fig. 10. We have included spin assignments resulting from this work and the assignments of other investigators where we have data which is consistent with the earlier assignments. No cases are known to us of earlier assignments in conflict with the present results. Table III provides mixing ratios for the 1440- and 1619-keV transitions which are in excellent agreement with previous determinations⁸ of them. Branching ratios are included in Fig. 10. This figure and Tables I and III are a reasonably complete summary of the results of this experiment.

COMPARISON OF LEVELS WITH MODEL CALCULATIONS

The only detailed calculations which might be tested by these results are the mixed-configuration calculations of Lips and McEllistrem,² which include configurations with only one proton excited outside the $f_{7/2}$ shell. Up to about 2-MeV excitation, the calculations fit rather well; the second $\frac{3}{2}^-$ level is in about the right position and the number of levels below that energy is nearly correct. Above this energy, however, the model seems to have large deficiencies which set in rather abruptly. For example, the separation between $\frac{9}{2}^-$ levels is badly represented and the number of calculated levels between 2- and 3.5-MeV excitation energy is only about $\frac{1}{2}$ of those observed. With such deficiencies above 2-MeV excitation, it is interesting to note that not only are the lower levels correctly positioned by the model, but $M1$, $E2$ mixing ratios for their decay and recently measured nuclear lifetimes in ^{53}Mn are quite well represented.³⁴

CONCLUSIONS AND SUMMARY

The study of the $^{53}\text{Cr}(p,n)^{53}\text{Mn}$ and $^{53}\text{Cr}(p,\gamma)^{53}\text{Mn}$ reactions has given a considerable amount of new information about the level and decay schemes of ^{53}Mn . Excitation energies of 21 excited states were measured, most of them resulting from measurements of neutron and γ -ray energies. Results of the two types of measurements agreed to within 1 or 2 keV, and uncertainties of ± 2 keV are attached to the excitation-energy determinations.

Two groups of close-lying levels have been resolved in the neutron spectra, a triplet at 2669, 2685, and 2705 keV and a doublet at 3095 and 3124 keV. These separations illustrate the resolution capability in neutron spectra using this technique.

The WHF statistical-model formalism has provided a good representation of the measurements for proton energies near or above 5 MeV. Away from analog resonances the neutron angular distributions and absolute (p,n) cross sections agree well with predictions of the model. For the cal-

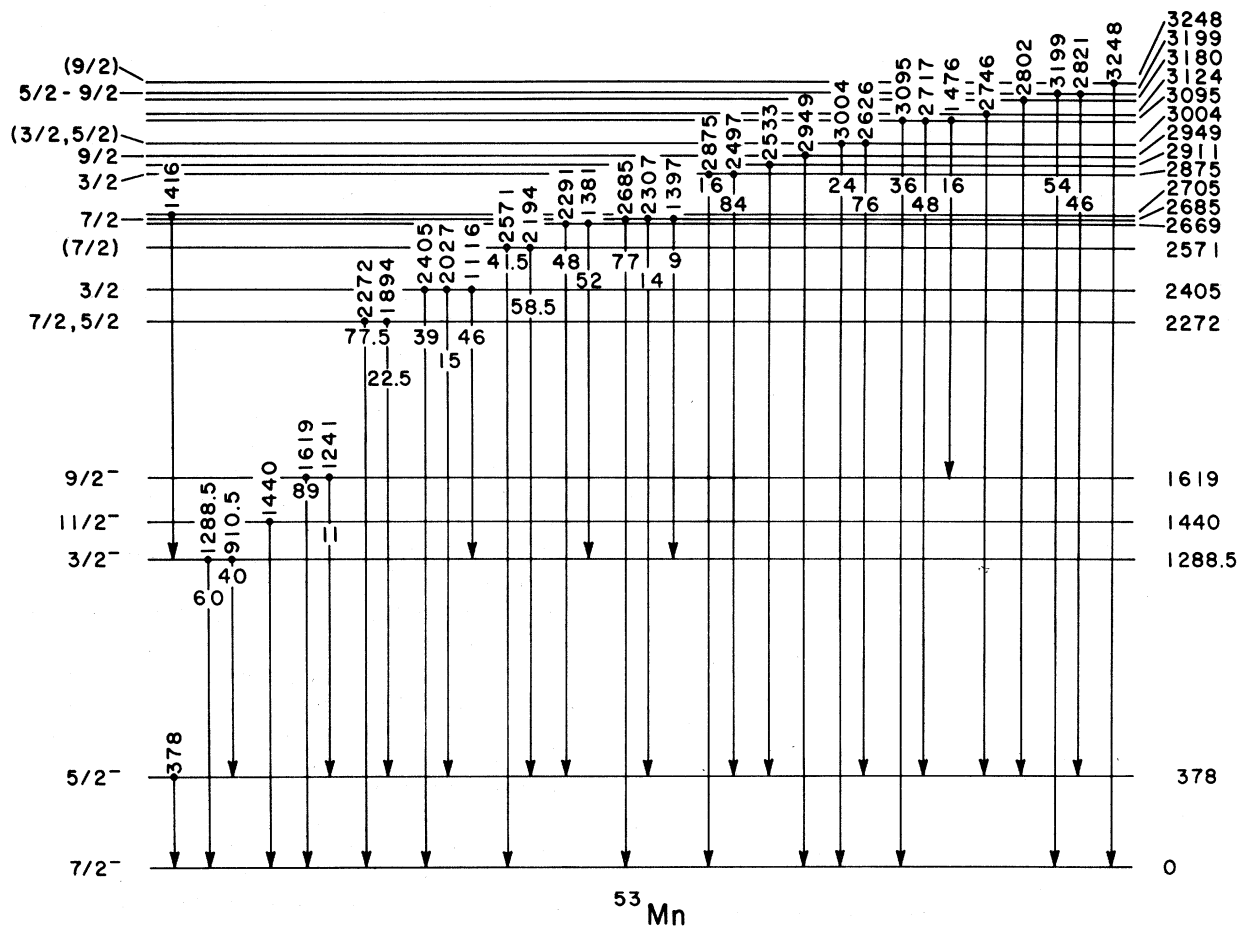


FIG. 10. Level and decay scheme for ^{53}Mn . Excitation energies above 2 MeV are accurate to ± 2 keV. Branching-ratio accuracies are given in Table I.

culations, the Rosen global-fit potentials were used without parameter adjustment or other modification. The γ -ray angular distributions are consistent with predictions of the formalism over a wide range of proton energies, but these are quite insensitive to details of the reaction mechanism. The success of the formalism and the availability of both neutron and γ -ray angular distributions permitted firm spin assignments to a few levels and probable assignment to others, as indicated: 2272 keV, $\frac{5}{2}$ or $\frac{7}{2}$; 2405 keV, $\frac{3}{2}^-$; 2571 keV, $(\frac{7}{2})$; 2685 keV, $\frac{7}{2}$; 2949 keV, $\frac{9}{2}$; 3004 keV, $(\frac{3}{2}^+, \frac{5}{2}^+)$; 3199 keV, $\frac{5}{2}-\frac{9}{2}$; and 3248 keV, $(\frac{9}{2})$.

Mixed-configuration shell-model calculations including only proton excitations and allowing only one proton excited out of the $f_{7/2}$ shell represent

level energies and electromagnetic transition rates very well below about 2-MeV excitation, but the success of the model deteriorates rapidly above that energy.

ACKNOWLEDGMENTS

The authors are indebted to Dr. Thomas B. Grandy, now of Windsor University, Ontario, for his contributions and advice in optimizing the time resolution of the neutron-detection system and the (p, n) measurements and their analysis. We wish also to thank J. J. Egan, M. R. McPherson, and other members of the Nuclear Structure Laboratory staff for their assistance in taking the data. The aid of the University of Kentucky Computing Center is acknowledged.

*Work supported in part by the National Science Foundation.

†Present address: Shawnee College, Ullin, Illinois 62992.

¹J. D. McCullen, B. F. Bayman, and E. Kashy, *Phys. Rev.* **134**, B513 (1964).

²K. Lips and M. T. McEllistrem, *Phys. Rev. C* **1**, 1009 (1970).

³D. D. Armstrong and A. G. Blair, *Phys. Rev.* **140**, B1226 (1965).

⁴B. J. O'Brien, W. E. Dorenbusch, T. A. Belote, and J. Rapaport, *Nucl. Phys.* **A104**, 609 (1967).

⁵B. Cujec and I. Szöghy, *Phys. Rev.* **179**, 1060 (1969).

⁶S. E. Arnell and S. Sterner, *Phys. Letters* **9**, 319 (1964).

⁷P. H. Vuister, *Nucl. Phys.* **83**, 593 (1966); **A91**, 521 (1967).

⁸M. T. McEllistrem, K. W. Jones, and D. M. Sheppard, *Phys. Rev. C* **1**, 1409 (1970).

⁹D. D. Armstrong, A. G. Blair, and H. C. Thomas, *Phys. Rev.* **155**, 1254 (1967).

¹⁰E. Newman and J. C. Hiebert, *Nucl. Phys.* **A110**, 366 (1968).

¹¹B. Cujec, R. Dayras, and I. Szöghy, *Bull. Am. Phys. Soc.* **13**, 723 (1968).

¹²A. J. Elwyn, H. H. Landon, S. Oleksa, and G. N. Glasoe, *Phys. Rev.* **112**, 1200 (1958).

¹³G. Brown, S. E. Warren, and R. Middleton, *Nucl. Phys.* **77**, 365 (1966).

¹⁴S. Tanaka, P. H. Stelson, W. T. Bass, and J. Lin, *Phys. Rev. C* **2**, 160 (1970).

¹⁵W. Hauser and H. Feshbach, *Phys. Rev.* **87**, 366 (1952).

¹⁶H. J. Kim and R. L. Robinson, *Phys. Rev.* **162**, 1036 (1967).

¹⁷G. C. Dutt and F. Gabbard, *Phys. Rev.* **178**, 1770 (1969).

¹⁸J. J. Egan, G. C. Dutt, J. E. Wiest, and F. Gabbard, to be published.

¹⁹A. O. Hanson and J. L. McKibben, *Phys. Rev.* **72**, 673 (1947).

²⁰J. J. Egan, G. C. Dutt, M. McPherson, and F. Gabbard, *Phys. Rev. C* **1**, 1767 (1970).

²¹D. E. Velkley, K. C. Chung, A. Mittler, J. D. Brandenberger, and M. T. McEllistrem, *Phys. Rev.* **179**, 1090 (1969).

²²D. A. Gedcke and W. J. McDonald, *Nucl. Instr. Methods* **58**, 253 (1968).

²³C. H. Johnson, C. C. Trail, and A. Galonsky, *Phys. Rev.* **136**, B1719 (1964).

²⁴J. B. Marion, *Rev. Mod. Phys.* **38**, 660 (1968).

²⁵J. W. Tepel, *Nucl. Instr. Methods* **40**, 100 (1966).

²⁶W. R. Smith, Oak Ridge National Laboratory Report No. ORNL-TM-930, 1964 (unpublished); and private communication.

²⁷L. Rosen, in *Nuclear Structure Study with Neutrons*, edited by N. de Meevergnies, P. Van Assche, and J. Verrier (North-Holland, Amsterdam, 1966), p. 379.

²⁸P. A. Moldauer, *Nucl. Phys.* **47**, 65 (1963).

²⁹F. G. Perey, *Phys. Rev.* **131**, 745 (1963).

³⁰F. Perey and B. Buck, *Nucl. Phys.* **32**, 353 (1962).

³¹K. C. Chung, private communication.

³²H. J. Rose and D. M. Brink, *Rev. Mod. Phys.* **39**, 306 (1967).

³³I. M. Szöghy, B. Cujec, and R. Dayras, private communication; and to be published.

³⁴K. Lips, private communication; and to be published.